LA-2202

C-13

LOS ALAMOS SCIENTIFIC LABORATORY

OF THE UNIVERSITY OF CALIFORNIA o LOS ALAMOS NEW MEXICO

MAGNETIC COMPRESSION OF SHOCK PREHEATED PLASMA

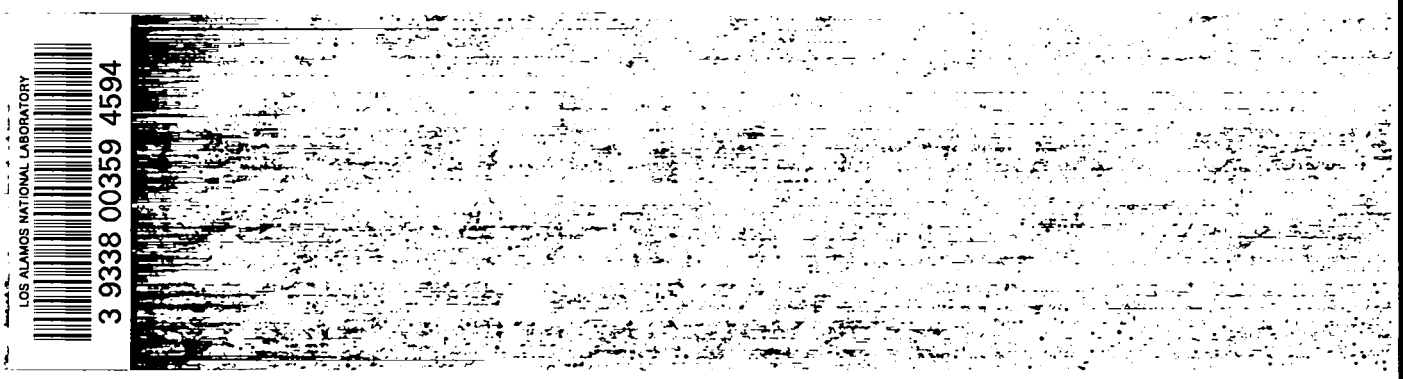

Printed in USA. Price $1.25. Available from the

Office of Technical Services
U. S. Department of Commerce
Washington 25, D. C.

LA-2202
CONTROLLED THERMONUCLEAR PROCESSES
(TID-4500, 13th ed., rev.)

LOS ALAMOS SCIENTIFIC LABORATORY
OF THE UNIVERSITY OF CALIFORNIA LOS ALAMOS NEW MEXICO

REPORT WRITTEN: April 1958

REPORT DISTRIBUTED: October 21, 1958

MAGNETIC COMPRESSION OF SHOCK PREHEATED PLASMA

by

Edward M. Little
David B. Thomson

Contract W-7405-ENG. 36 with the U. S. Atomic Energy Commission

ABSTRACT

In the experiments described, plasma was produced by the passage of planar shocks down the axis of a cylindrical discharge tube. The resulting plasma had a temperature of several electron volts.

A strong axial magnetic field which compressed and adiabatically heated the shock preheated plasma was then applied to the cylindrical section of the discharge tube.

One of the critical conditions of the experiment was that the preheated plasma had to have sufficient temperature and electrical conductivity so that the axial magnetic field would push on the plasma rather than diffuse through it, in the rise time of the magnetic field. The results presented here indicate that this condition was achieved and that the adiabatic heating obtained from the magnetic compression stage was in reasonable agreement with theoretical predictions over most of the range of temperatures and pressures covered.

ACKNOWLEDGMENTS

The authors would like to make the following acknowledgments. The condenser bank and associated power supplies and trigger circuits used for this experiment were inherited from the shock preheated pinch experiment (Totempole I), and were designed and constructed by R. S. Dike and A. E. Schofield, who were also instrumental in the design of the multiple spark gap.

The smear pictures were taken with the invaluable aid of W. P. Basmann.

Keith Boyer and W. C. Elmore gave many helpful suggestions which aided the writing of this report.

Many helpful discussions with F. R. Scott contributed to the development of the theory and the planning of the early phases of the experiment. The constructive participation of W. M. Bullis aided the interpretation of the shock theory.

The authors are especially indebted to Vernal Josephson, whose support and enthusiasm made the experiment possible.

CONTENTS

ILLUSTRATIONS

CONTENTS
(cont'd)

I. Introduction

This study[1] of the compression and heating of a hot plasma by an axial magnetic field involved a two-stage experiment. First, hot plasma was obtained by directing high-velocity planar shocks down the axis of a cylindrical discharge tube. Second, a high-intensity axial magnetic field which compressed and further heated the plasma was applied. This work was done during the late spring and summer of 1957.

II. The Production of Hot Plasma by Fast Shocks

The ability of fast planar shocks in deuterium to produce plasma of sufficient conductivity to be confined by an axial magnetic field has been studied[2] for the case of shocks produced by a tapered pinch tube called the wineglass.

In the studies reported here, planar shocks were produced in a tapered tube driven by a rapidly varying axial magnetic field. Previously, such an oscillating B_z field had been used to produce radial shocks, as observed at Los Alamos in experiments with the "Jug,"[3] and with "Gloworm."[4] In these cases, rapidly oscillating magnetic and electric fields comprised the initial energy source. We shall call these "$\dot{B}_z$" fields, to distinguish them from fields which are used for their magnetic pressure alone. The radial shocks result from the rapid build-up of an I_θ current, which in turn results from the sudden breakdown of the gas. The breakdown is due to the electric field E_θ associated with the $\dot{B}_z$. The electric field is greatest near the outer region of the gas so a radial shock starts there and moves inward. One may think of this motion as caused by a

combination of the magnetic pressure due to the B_z field, which builds up with time, and the joule heating, which suddenly increases the temperature of the gas in the outer region. Data from the "Gloworm"[4] experiment indicated plasma had been produced of at least 5 to 10 ev temperature.

A. The Tapered $\dot{B}_z$ Shock Tube

The smear pictures of the radial shocks or compressions produced by $\dot{B}_z$ fields have many similarities with the smear pictures of the radial shocks and compressions produced by pinch currents. Hence it was decided to see if the tapered-tube principle as employed in the wineglass experiments[2,5] could be combined with the $\dot{B}_z$ method to produce planar shocks in the axial direction. This method of magnetically producing shocks was first tried by Ferrell,[6] who used several parallel three-turn coils driven by a 10 μf capacitor charged to 5 kv. He observed shock velocities of 1 to 3 cm/μsec in the adjacent linear tube.

The tapered-tube $\dot{B}_z$ method has the important advantage of eliminating electrodes and results in a considerable simplification of the hardware. In addition, it results in an order-of-magnitude reduction in impurities.

Figure 1 is a photograph of one of the arrangements used in the adiabatic heating study described in Section III. The bottom section of the discharge tube was a tapered section, complete with $\dot{B}_z$ coils, used to produce hot plasma for the study of adiabatic heating.

The $\dot{B}_z$ field was produced by three parallel two-turn coils spaced about 2 in. apart along the tapered section. The coils were connected in parallel to a coaxial spark gap, which in turn was connected to twelve 25 kv capacitors by 24 parallel lengths of RG/8U coaxial cable. The tapered section of the discharge tube was 7 in. long. The maximum diameter was 4 in. (o.d.), the minimum diameter 1-1/2 in. (o.d.), the taper angle about 10°, and the wall thickness 1/4 in. The length of the adjacent linear section of the tube was 6-1/4 in.

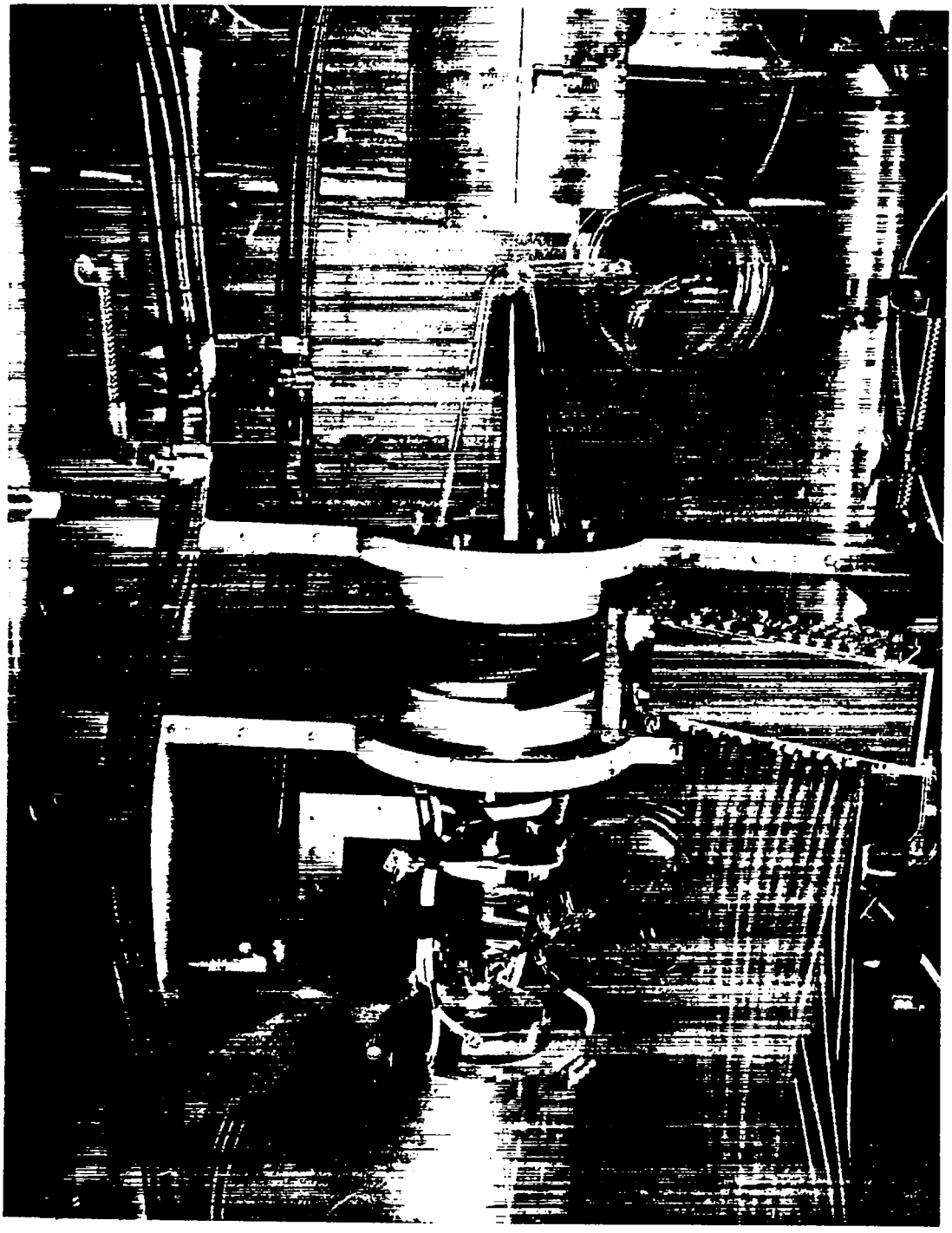

Fig. 1 Totempole II, showing shock-producing coils and two-turn main compression coil made from 1/2 in. brass rod.

The voltage V_θ produced by the $\dot{B}_z$ coils was measured with a one-turn pick-up loop, wound on the outside of the discharge tube. By measuring the frequency and magnitude of the V_θ signal, and knowing the area of the pick-up loop, one can calculate the magnitude of the enclosed B_z field. The V_θ signal was measured at both the narrow and wide ends of the tapered tube, as well as at the center.

In a typical case, the period of the oscillating B_z field was found to be 11.6 μsec. The maximum voltage signal V_θ was 2.7 kv at both the narrow and wide ends of the tube. This means that the E_θ field was greatest at the narrow end of the tube and one would expect the breakdown of the gas to occur there first.

The maximum current supplied by the 12 μf capacitor bank when charged to 20 kv was computed to be 130,000 amp. The total inductance was 0.28 μh. The inductance of the three two-turn coils in parallel was 0.075 μh, the remainder of the inductance being in the external circuit. Under these conditions the maximum B field was 7500 gauss at the wide coil and 30,000 gauss at the narrow coil. A one-turn shorting coil, placed at the junction of the straight and tapered sections of the discharge tube served to isolate the shock-producing coils from the main adiabatic compression coil, whose use is described later.

Smear pictures were taken of both velocity and profile of the shocks produced by the arrangement described. The smear camera was focused at the center of the linear section of the tube away from the $\dot{B}_z$ fields. Figure 2 shows a typical shock velocity picture. Such pictures in general show several distinct shock fronts, the earliest one having a typical velocity of about 4.4 cm/μsec. This front corresponds to the half cycle of E_θ during which the gas breaks down. This and later shock fronts decreased in velocity along the length of the tube seen by smear camera (11.75 cm), indicating considerable attenuation of the shock energy. The second shock front, having a much more constant velocity than the first, corresponds in time to the next half cycle of E_θ, and had a velocity of 8.8 cm/μsec for the case shown. It is, of course,

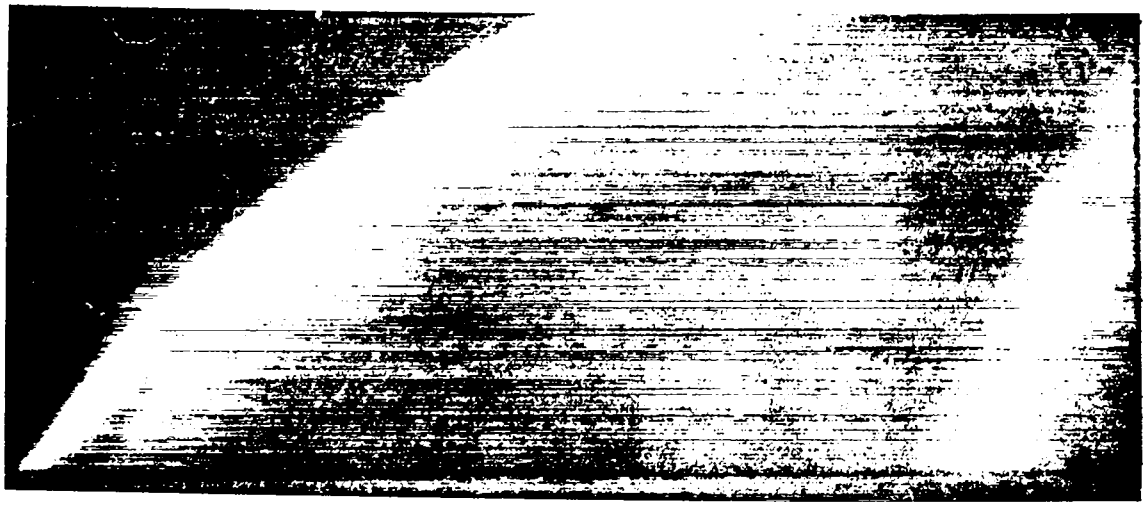

Fig. 2 Smear camera pictures of typical linear shocks.

Fig. 3 Smear camera picture showing radial profile of typical linear shocks.

traveling in gas heated by the earlier shock. Figure 3 shows the radial profiles of similar shocks, with the smear camera writing speed the same as for Fig. 2.

The shock velocities reported above occurred at a pressure of about 300 microns with the capacitor bank at 20 kv. The observed shock velocities decreased slowly with increase in deuterium pressure. The shock velocity increased slowly with capacitor voltage in the range 15 to 25 kv.

With the coil arrangement described, the tube could be fired at pressures of about 1000 microns down to pressures of less than 10 microns. This was a distinct advantage over the wineglass electrode arrangement, which with the same condenser bank would not fire at pressures lower than 25 microns.

B. Temperature Estimates from Shock Theory

The determination of plasma temperature from shock theory was not as straightforward for shocks produced in the tapered $\dot{B}_z$ tube as it was for shocks produced in the wineglass pinch tube. In the case of the wineglass, a single shock wave was produced, with smear pictures showing a well-defined front of the type used for the theoretical calculation* of temperature behind a shock front.

In the case of the $\dot{B}_z$ tube the measured velocity of the first shock indicated a temperature of only 3 to 4 ev according to shock theory. The second shock, corresponding to the next half cycle of E_θ, had a more constant velocity in the range 8 to 10 cm/μsec. Such a velocity would seem to imply a temperature of 7 to 10 ev. The second shock front, however, was traveling in the hot ionized gas produced by the first shock and hence the theoretical curves connecting shock velocity to temperature behind the shock do not apply. The fact that smear pictures show the

---

*The calculations were made by D. Venable and L. Stein and are published in Ref. 2.

second shock to be less intense than the first indicates that the gas was still considerably ionized when the second shock reached it.

If one thinks of a shock front as a continuing source of energy heating the gas as it goes along, one might suppose that a given shock velocity in a hot gas would create a hotter plasma than the same shock velocity in a cold gas. One would then conclude that the second shock observed in the present experiments heated the plasma even hotter than 7 to 10 ev value predicted by shock theory.

On the other hand, since the velocity of sound is faster in a hot gas than at room temperature, the Mach number assigned to a shock of given velocity will be smaller for a shock in a hot gas than in cold gas; hence the curves of Venable and Stein would predict a lower temperature. It should be noted that the radial smear picture of the second shock indicates a much more diffuse shock front than that used in the theory.

Thus for multiple shocks, shock theory should be expected to give us only a rough estimate of the plasma temperature. However, from other considerations (see Section III), the temperature in the tube, T_o, at the start of the main compression field agrees well with the temperature behind the first shock front as predicted by shock theory.

C. Use of a Copper Sheet for the $\dot{B}_z$ Coil

In an effort to achieve stronger shocks, the three parallel two-turn coils were replaced by a single copper sheet 5.75 in. long. The sheet fitted the tapered tube snugly so that it had the same taper angle. The sheet was connected to the spark gap by two short 1 in. wide straps held flat against each other to reduce inductance. The spark gap and capacitor bank assembly was the same one as used with the parallel coils.

The $\dot{B}_z$ period with the sheet coil was 8.5 μsec, compared with 11.6 μsec for the parallel coil. The faster $\dot{B}_z$ field gave about the same shock velocity as did the slower $\dot{B}_z$ field of the parallel coils. The shock fronts looked very similar for the two cases.

D. Use of Two Tapered $\dot{B}_z$ Sections

Since the purpose of the tapered $\dot{B}_z$ section of the discharge tube was to produce a hot plasma in the linear section of the tube, the complete discharge tube was made with an identical tapered section on each end of the linear section, as shown in Figs. 1, 4, 5, and 7. For the experimental data reported here, and in Section III, the one-turn copper sheet coil was used for the bottom $\dot{B}_z$ section, and the three parallel two-turn coil arrangement was used for the top $\dot{B}_z$ section. Each coil was connected separately to an identical spark gap and capacitor bank.

One of the characteristics of the $\dot{B}_z$-produced discharge is that the gas ordinarily does not break down on the first half cycle. Earlier data[4,7] with $\dot{B}_z$-induced discharges showed that, in many cases, several half cycles of V_θ are necessary to build up a level of electron density sufficient to enable a succeeding half cycle of V_θ to break down the gas at zero B field. Only after the gas breaks down does it achieve sufficient conductivity for magnetic fields to compress it, or for joule ($j_\theta^2 \rho$) heating to be appreciable.

The gas did not break down with the tapered shock-driving sections until the second or third half cycle of V_θ, depending on the voltage, pressure, period, etc. This is a disadvantage because of the logarithmic decay of the oscillating field.

In the results reported in Section III, the top shock coil was excited first, and the resulting shock used to preheat the gas in the bottom shock section. Then the bottom shock coil (the copper sheet) was excited so that the first quarter cycle of V_θ and the corresponding half cycle of B_z could act on a hot plasma. The result was to increase the velocity of the first shock produced by the bottom section from about 4.0 cm/μsec for no preheating to 5.5 cm/μsec when preheating was used.

Figure 6 shows scope traces of the V_θ pulse at the bottom shock section for the case of no preheating and the case of preheating from

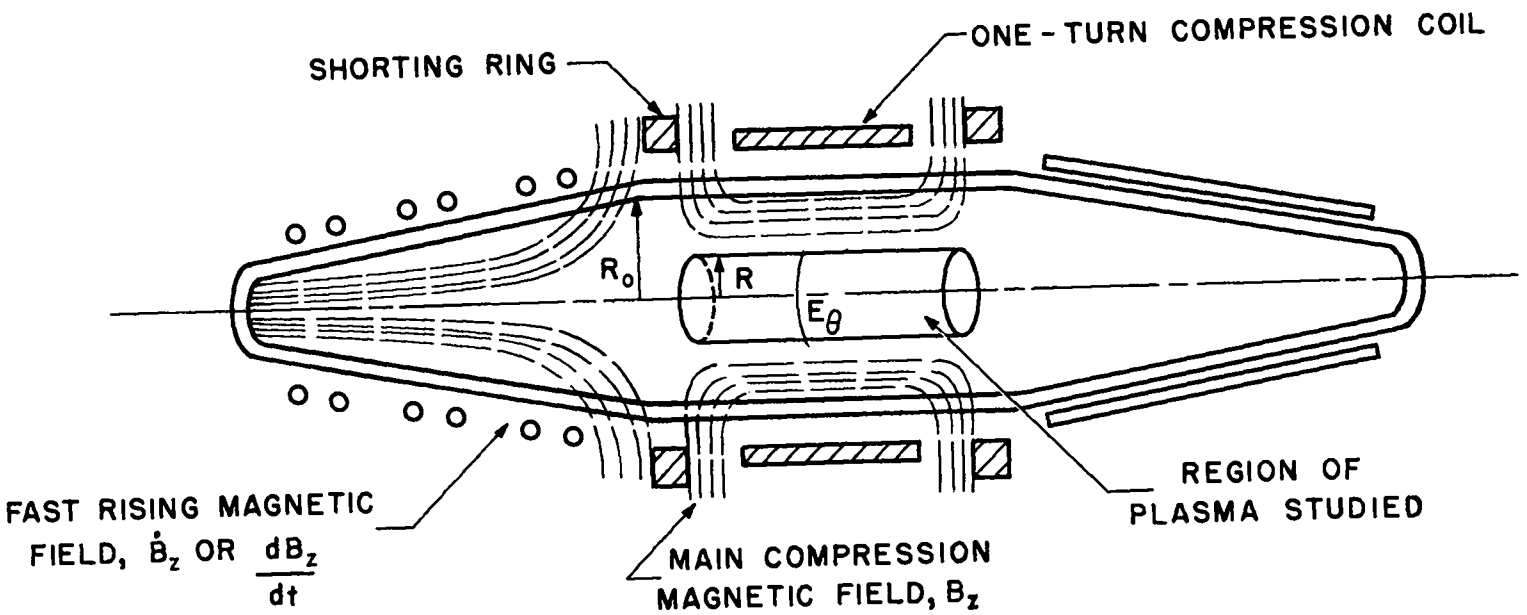

Fig. 4 A sketch of the tube showing the shock-producing $\dot{B}_z$ field, the main compression B_z field, and the general region of plasma studied.

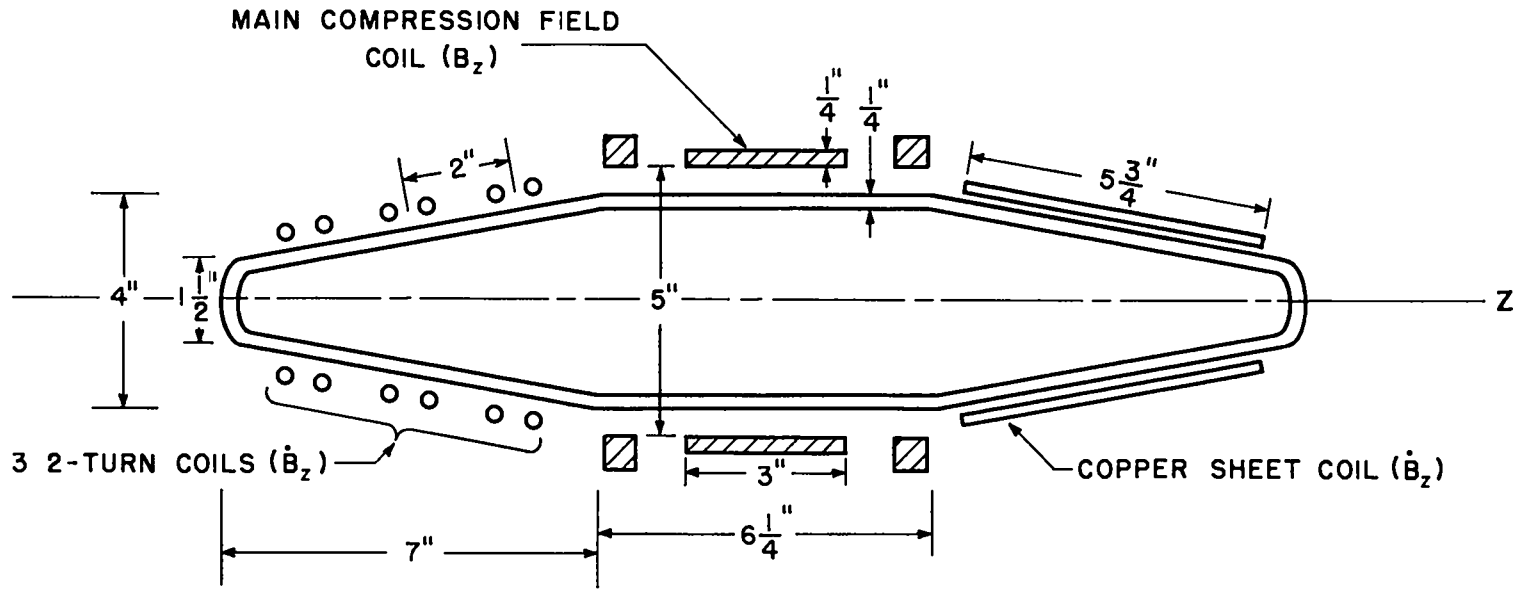

Fig. 5 A sketch showing dimensions of the tube and coils.

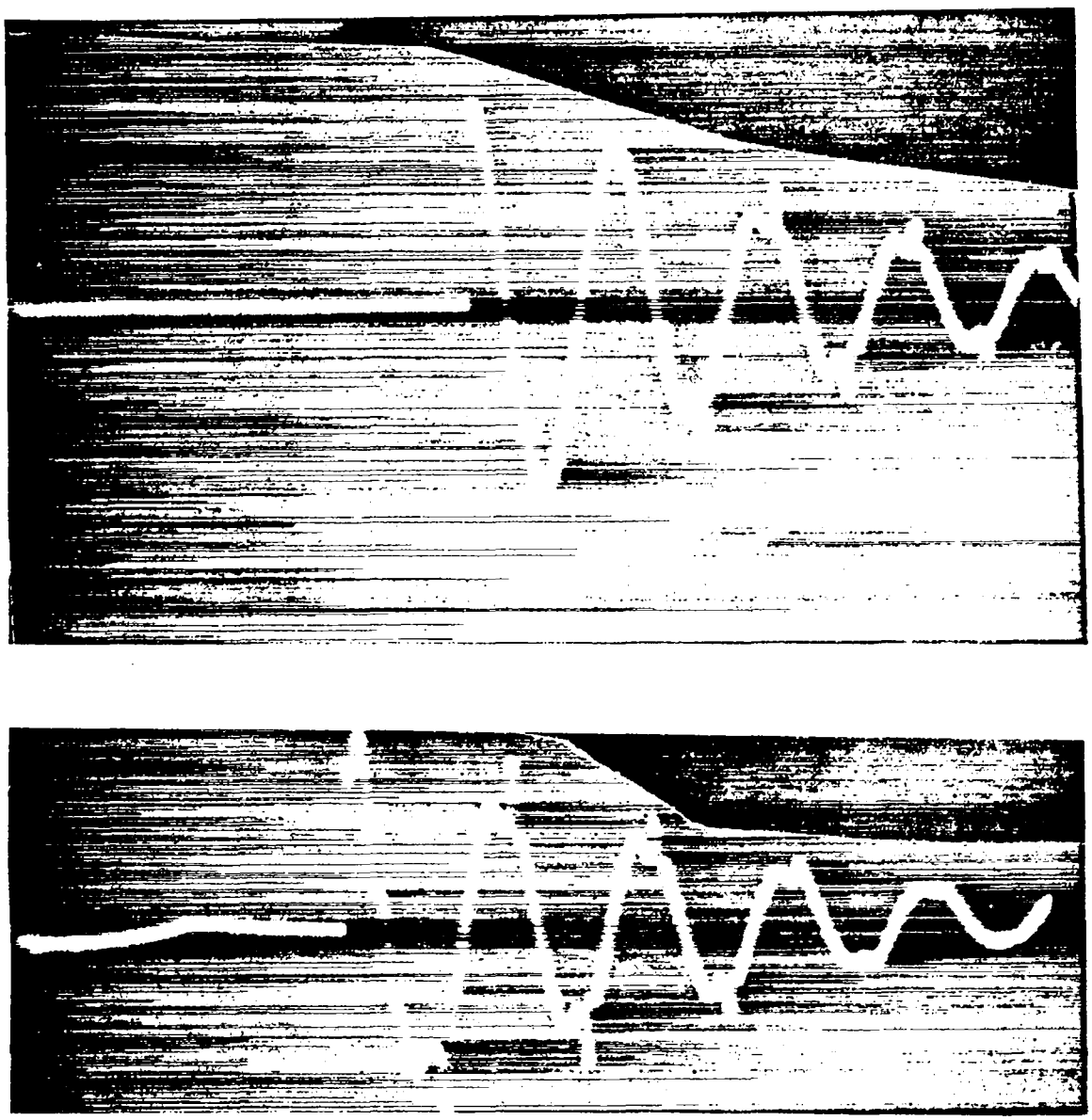

Fig. 6 Scope traces of the V_θ pulse at the lower shock section. The top photo shows the pulse when the lower section was not preheated. The bottom photo shows the pulse when the lower section was preheated by shocks from the upper shock tube.

the top shock section. The perturbations from a pure sine wave give a good indication as to whether or not there is hot plasma enclosed by the $\dot{B}_z$ coil at any given half cycle.

The use of two shock sections resulted in the production of a hot plasma in the entire discharge tube, but the mechanism of heating was so complex that deductions from simple shock theory were very difficult. About all one could say at this point was that the plasma temperature in the linear section resulting from the several shocks must have been of the order of several electron volts shortly after the passage of the shock fronts.

III. Magnetic Compression and Adiabatic Heating

This experiment was designed to study the adiabatic heating mechanism at densities and temperatures of interest to the Sherwood program, which has as its goal to heat plasma to thermonuclear temperatures.

Adiabatic compression of preheated plasma has been done most commonly at this laboratory in pinch tubes.[8,9] In these devices, a B_θ compressing field is obtained from the pinch current itself. This method has the advantage of producing an intense magnetic field near the outer radius of the pinch. A disadvantage of the method in straight tubes is the necessity for electrodes to supply the pinch current. Large quantities of impurities are observed on the walls of pinch discharge tubes after a few shots, and the electrode surfaces generally appear sufficiently corroded to have been the main source of impurities.

In many cases impurities may have been sufficient to appreciably change the effective value of particle density N_o used in pressure-balance calculations. In addition, impurities represent an energy sink distributed throughout the hot gas. The shock channeling data[2] strongly suggested the feasibility of using an externally produced increasing B_z field to accomplish the adiabatic compression of a preheated plasma. This method

has the following advantages:

1. The elimination of electrodes to supply the compressing field greatly reduces impurities.
2. The B_z compressing field should form a reasonably stable "container" for the hot plasma, as it did in the shock channeling experiments.

In this experiment, a high-energy B_z field was applied at the linear section of the tube shown in Fig. 7. The gas was preheated by the multiple shocks described in Section II. This combined arrangement is called Totempole II.

A. Adiabatic Heating Theory

The adiabatic heating theory for the Totempole II experiment is based on the following equations:

$$PV^{\gamma} = \text{constant} \quad (1)$$

$$P = NkT \quad (2)$$

$$NV = \text{constant} \quad (3)$$

where

P = gas pressure
V = gas volume
T = absolute temperature
γ = ratio of the specific heats (c_p/c_v)
k = Boltzmann constant
N = number of particles (ions and electrons) per unit volume

These equations, together with the magnetic pressure balance equation

$$\frac{B^2}{8\pi} = NkT \quad (4)$$

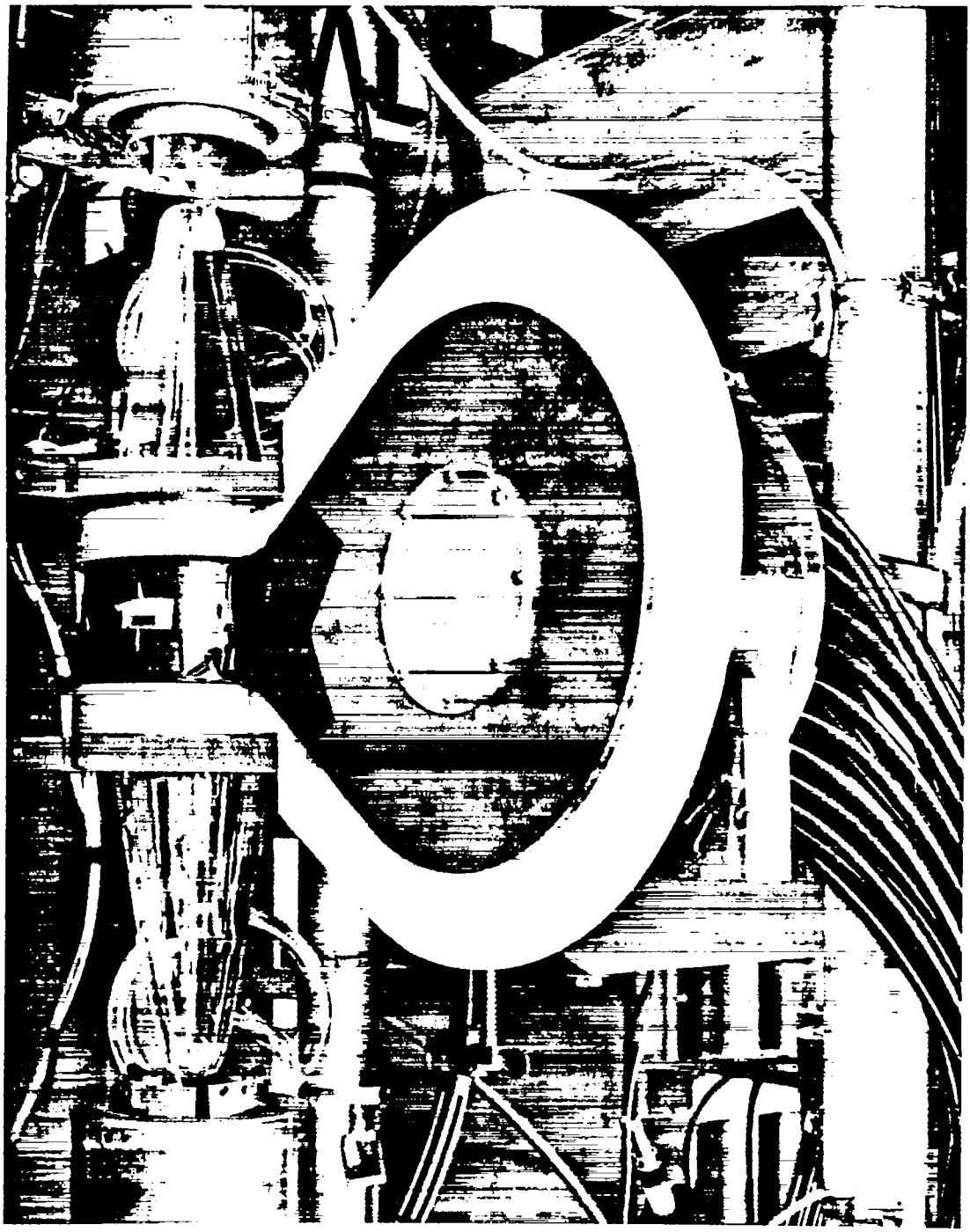

Fig. 7 Totempole II arrangement, showing the one-turn copper band main compression coil.

where B is the magnetic flux density, can be combined to give the equations

$$kT_f = kT_o\left(\frac{V_o}{V_f}\right)^{(\gamma-1)} \tag{5}$$

$$\frac{B_f^2}{8\pi} = N_o kT_o\left(\frac{V_o}{V_f}\right)^{\gamma} \tag{6}$$

where the subscripts f and o correspond to final and initial states of the heating process. By eliminating the ratio V_o/V_f from Eqs. (5) and (6), one obtains

$$kT_f = kT_o\left(\frac{B^2}{8\pi}\frac{1}{N_o kT_o}\right)^{(\gamma-1)/\gamma} \tag{7}$$

Since $\gamma = 5/3$ for a deuterium plasma of sufficient collision rate, Eq. (7) becomes

$$kT_f = \frac{(kT_o)^{3/5}B_f^{4/5}}{(8\pi N_o)^{2/5}} \tag{8}$$

Equation (8) predicts the final temperature that will be reached for a given initial temperature, initial density, and a given final value of the compressing B field. It is interesting to observe that the final temperature predicted by Eqs. (7) and (8) does not depend on whether the volume change accompanying the compression is in one, two, or three dimensions.

The following conditions must be met if the ideal adiabatic heating equations are to describe the experiment correctly:

(a) The initial electrical conductivity of the plasma must be high enough so that the magnetic field will push on the plasma rather than diffuse through it. It has been shown that plasma with initial temperatures of the order of several ev will reasonably meet this requirement.

Since conductivity goes as $T^{3/2}$, higher initial temperatures, of course, would be very desirable.

(b) A Boltzman temperature for both the electrons and ions must exist and these temperatures must be the same.

Condition (b) will be met if the relaxation times for the following three types of collision processes are short compared with the compression and confinement times of the experiment:

1. Electron-ion collision.
2. Ion-ion collision.
3. Electron-electron collision.

Spitzer,[10] in considering these relaxation times, defines a "self-collision time" t_c for a group of particles interacting with each other to approach a Boltzmann distribution. He also defines an "equipartition time" t_{eq} as the time for two groups of particles at different initial Boltzmann temperatures to approach the same temperature.

If one assumes an electron-deuteron gas, of density 10^{15} particles/cm^3 and temperature 10 ev, one obtains values of t_c of the order of 0.05 μsec for deuterons, and less than 0.001 μsec for electrons from Spitzer's formula. Since both t_c and t_{eq} are proportional to $T^{3/2}/N$, and since for an adiabatic compression with $\gamma = 5/3$, Eqs. (3) and (5) show that $T^{3/2}/N$ is an invariant, the relaxation times remain unchanged during compression. Since we are dealing with confinement and compression times of the order of 1 to 10 μsec, these self-collision times are sufficiently short to ensure Boltzmann distributions of the ions and of the electrons.

The equipartition time t_{eq} calculated from Spitzer's formula comes out to be of the order of 1 or 2 μsec for the same temperature and density. Since there is no reason why the electron and ion temperatures should separate very much during compression, a compression time of 10 μsec should be sufficiently long to maintain equipartition.

(c) The loss due to radiation must be negligible. The radiation loss problem is present in most Sherwood devices and generally has been estimated to be unimportant at temperatures below 1 kev. If the impurity

level is high enough, as may be the case with electrodes, radiation would be important. However, in the electrodeless all-glass system used here, it is hoped that radiation from impurities is negligible.

(d) The diffusion of heat out the ends must be small. This condition is one of the most critical for the experiment. Spitzer[10] discusses the thermal conductivity K of fully ionized gases and shows that $K \propto T^{5/2}$. The heat diffusion loss out the ends increases drastically with the temperature.

The important parameter measuring heat loss is the diffusion time t_d in which temperature decays a given amount because of diffusion out the ends. Rough calculations based on Spitzer's formula indicate that for the lower densities and the higher temperatures considered, t_d may be less than 1 μsec; this would be seriously short compared with a 10 μsec compression time. At the higher initial densities and at temperatures of several tens of electron volts, estimated diffusion times are long enough compared with the compression time to prevent serious heat loss. The effect of heat diffusion will be further discussed later in this section.

B. Production of the Compression Field

A large capacitor bank containing 190 1-μf capacitors rated at 25 kv was used to supply energy for the compression field. Each capacitor was connected by a separate length of RG 8/U cable to a coaxial spark gap which in turn was connected to the B_z field coil. In the first arrangement tried, shown in Fig. 1, the B_z coil itself consisted of two turns of 1/2 in. diameter brass rod. The coil was held in place at the center of the straight section of the discharge tube by phenolic supports. Twenty-two 6 ft. lengths of RG 8/U cable connected the coil with the spark gap. With this coil, a B_z of 120,000 gauss was achieved when the condenser bank was operated at 20 kv. The V_θ voltage observed with a one-turn pick-up loop was 8 kv, hence the effective coil voltage was 16 kv, indicating that 80 per cent of the total inductance of the system

was in the coil itself. The oscillating period was 90 μsec so that the first quarter cycle of compression was 22.5 μsec.

The device was operated for a number of shots, complete with preheating, but before smear pictures could be taken, the B_z coil connection was severely damaged by mechanical forces produced by the high currents involved. Several less rugged coils were completely destroyed by magnetic forces before the coil of 1/2 in. brass rod shown in Fig. 1 was installed.

C. Multiple Spark Gap and Fast B_z Coil

Following this preliminary arrangement a multiple spark gap assembly was constructed to accomplish the following:

1. Reduce the external inductance so that a lower inductance B_z coil could be used. It was hoped that the faster rising B_z field would reduce the effect of diffusion losses.

2. Reduce the timing jitter in the firing of the main condenser bank.

3. Improve the voltage ranges over which the machine could operate.

4. Improve the general reliability of operation.

The multiple spark gap consisted of ten individual spark gaps spaced uniformly on a 24.0 cm radius circle. The ground return had a 27.5 cm radius. Although the peak current through the multiple gap could be as high as 700,000 amp, each individual gap had to carry only 70,000 amp. The lower current per gap increased the operating life over that of the single spark gap used previously for the same capacitor bank.

The adiabatic heating coil used with the multiple spark gap consisted of a one-turn copper sheet, of thickness 1/4 in., of diameter 5 in., and of length 3 in. It was held in place about the linear section of the tube by phenolic supports, and is shown in Figs. 4, 5, and 7. Figure 7 also shows the header and parallel cable arrangement used to

connect the coil with the multiple spark gap. The narrow radial slot cut in the center of the B_z coil sheet permitted radial smear pictures to be taken of the hot plasma in the tube. With 20 kv on the capacitor bank, a peak B_z field of just over 40,000 gauss was obtained with a rise time of 10 μsec. Figure 8 shows a scope trace of the B_z field, obtained by integrating the V_θ voltage picked up by a single-turn loop. The time markers are 5 μsec.

The ratio of the V_θ voltage to the capacitor bank voltage indicated that one half the total inductance of the system was in the B_z coil, and one half in the external inductance. The total inductance is computed from the oscillation frequency and capacitance to be 0.14 μh, so that the B_z coil itself had an inductance of about 0.07 μh.

The $\dot{B}_z$ coils for driving shocks were added to the tapered sections of the tube shown in Fig. 7 and the complete Totempole II experiment was performed. The bottom shock section was excited 25 μsec after the top shock section, and the compression section was then turned on 5 to 10 μsec later.

D. Discussion of Results

Measurements were made on Totempole II, varying the main capacitor bank voltage over the range 18 to 24 kv, and varying the D_2 pressure over the range 10 to 900 microns. A series of smear pictures was taken at each of three conditions:

1. With a capacitor voltage of 20 kv and D_2 pressure of 125 to 150 microns.

2. With a capacitor voltage of 20 kv and a D_2 pressure of 625 to 865 microns.

3. With a capacitor voltage of 20 kv and a D_2 pressure of 15 microns.

In addition, smear pictures were taken at 125 microns with only the main field bank used, i.e., no preheating shocks.

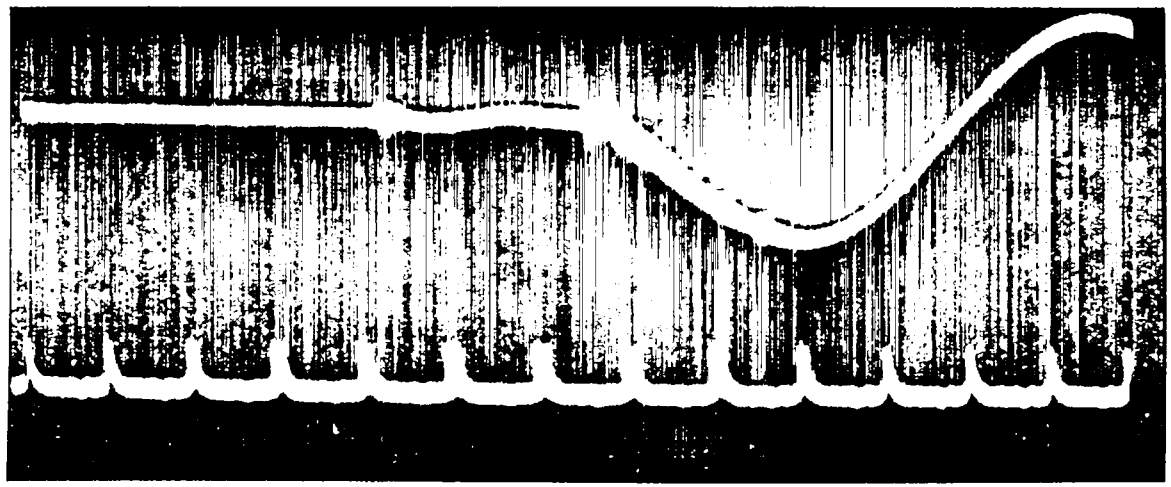

Fig. 8 Typical scope trace of the main B_z field. The markers are at 5 μsec intervals.

Figure 9 shows a typical smear picture of case (1), Fig. 10 for case (2), and Fig. 11 shows a smear picture for the case of no preheating by the tapered shock sections.

For the preheating cases, the smear pictures clearly show the compression of the hot plasma. The fact that a radial shock or implosion appears on the smear picture for the case of no preheating indicates that the E_θ field associated with the compressing B_z field must do considerable ionizing and heating on its own. The radial motion is seen to be much faster in the case of no preheating than in the preheating case. This behavior was similar to that obtained with the "Gloworm"[4] experiment.

The smear pictures may be analyzed in the following way. The compression recorded in the pictures is assumed to be cylindrical, so that the volume ratio V_o/V_f of Eq. (5) is $(R_o/R)^2$, where R_o is the initial radius of the gas (i.e., the inner radius of the tube) and R is the outer radius of the light recorded in the pictures. The radius R is assumed to be the outer radius of the hot plasma at any time. Then Eq. (6) may be written in the form

$$\frac{R_o}{R}^{5/3} = \frac{B}{(8\pi N_o k T_o)^{1/2}} \qquad (9)$$

where we have again taken $\gamma = 5/3$.

According to Eq. (9), a plot of $(R_o/R)^{5/3}$ versus B should give a straight line. The quantity $(8\pi N_o k T_o)^{1/2}$ represents the initial condition of the hot plasma and can be evaluated from the slope. The radius ratio R_o/R was read directly off the smear pictures at regular time intervals. The values of B corresponding to these same time intervals were obtained from a scope trace such as Fig. 8.

Figure 12 shows typical plots of $(R_o/R)^{5/3}$ versus B. Curve II is for normal Totempole II operation with shock preheating. The base deuterium pressure is 125 microns. As B varies from 0 to 40,000 gauss, the curve is a straight line within experimental error. Above 40,000 gauss, the values of $(R_o/R)^{5/3}$ appear to be a little larger than theory

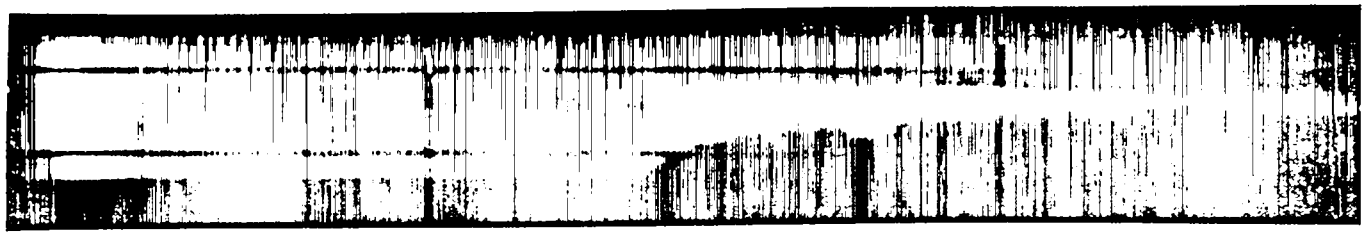

Fig. 9 Smear camera picture of the radial compression with capacitor bank charged to 20 kv and D_2 pressure of 125 microns. The time scale is the same as for Fig. 10.

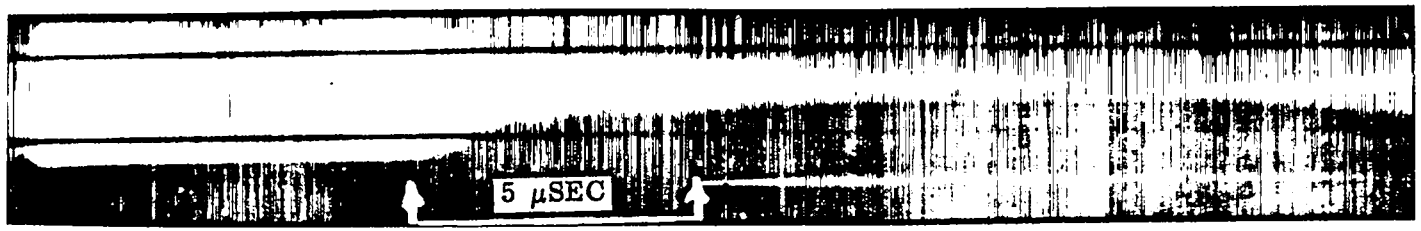

Fig. 10 Smear camera picture of the radial compression with capacitor bank charged to 20 kv and D_2 pressure of 625 microns.

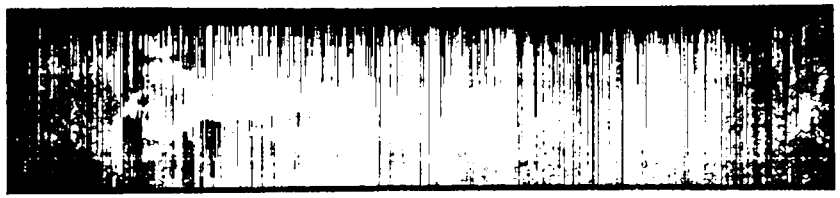

Fig. 11 Smear camera picture of the radial compression with no linear shock preheating and with D_2 pressure of 125 microns. The time scale is the same as for Fig. 10.

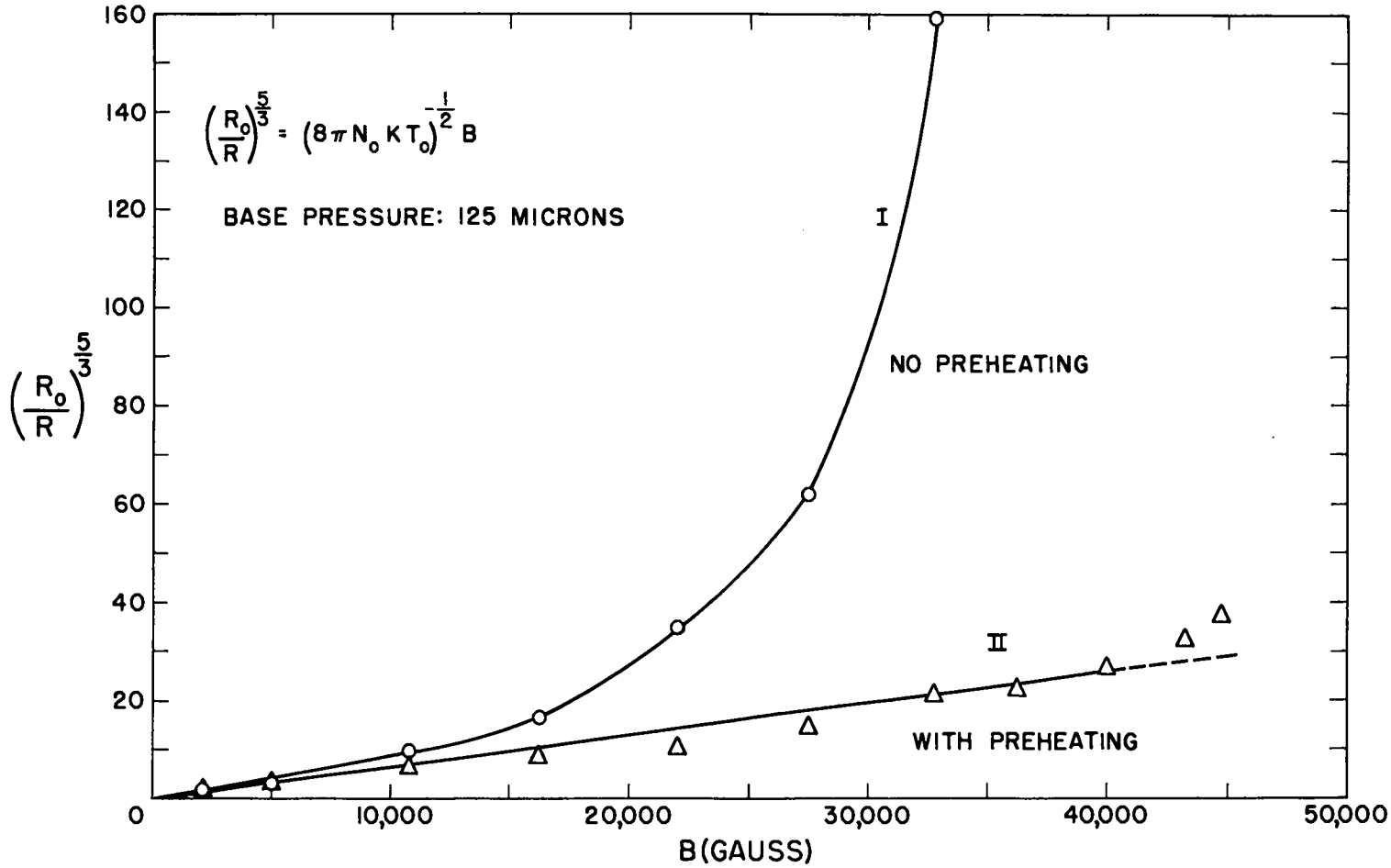

Fig. 12 Plots of $(R_o/R)^{5/3}$ as a function of B without shock preheating (Curve I) and with shock preheating (Curve II). The base pressure of deuterium was 125 microns.

would predict, indicating that there was some temperature loss. This could be due to diffusion out the ends. Curve I shows the same kind of plot for a case where the preheating shocks were not fired. As already mentioned, there is some effective "preheating" for this case due to the E_θ field of the compressing B field and hence a source of plasma to give Curve I. The fact that Curve I is definitely not a straight line but shows values of $(R_o/R)^{5/3}$ much larger than for Curve II illustrates the value of the preheating shocks.

Figure 13 shows typical plots of $(R_o/R)^{5/3}$ versus B for three different values of the initial base deuterium pressure. The same shock preheating was used in the three cases. Over the range of 0 to 40,000 gauss, all three curves appear to be straight lines within the experimental error. The curve for 15.5 microns deviates drastically from the theory just above 40,000 gauss, however.

The curves shown in Figs. 12 and 13 strongly indicate that the adiabatic heating theory presented here is applicable for the densities and temperatures covered. One would certainly expect it to be applicable at higher densities and for higher electrical conductivities.

At higher temperatures and at densities lower than 15 microns, one would expect deviations from the simple theory, since diffusion out the ends must then become serious. This trend is indicated by the 15.5 micron case of Fig. 13.

The slopes from the curves of Figs. 12 and 13 give values of initial energy density of the gas $N_o kT_o$. Since we have assumed pressure balance during the compression stage, the final energy density, taken here at 40,000 gauss in all cases, is just $B^2/8\pi$. A final temperature can be calculated from

$$kT_f = \frac{B_f^2}{8\pi N_o (R_o/R_f)^2}$$

where (R_o/R_f) is obtained from the curve at 40,000 gauss. If one assumes that the initial particle density is that computed from the base deuterium

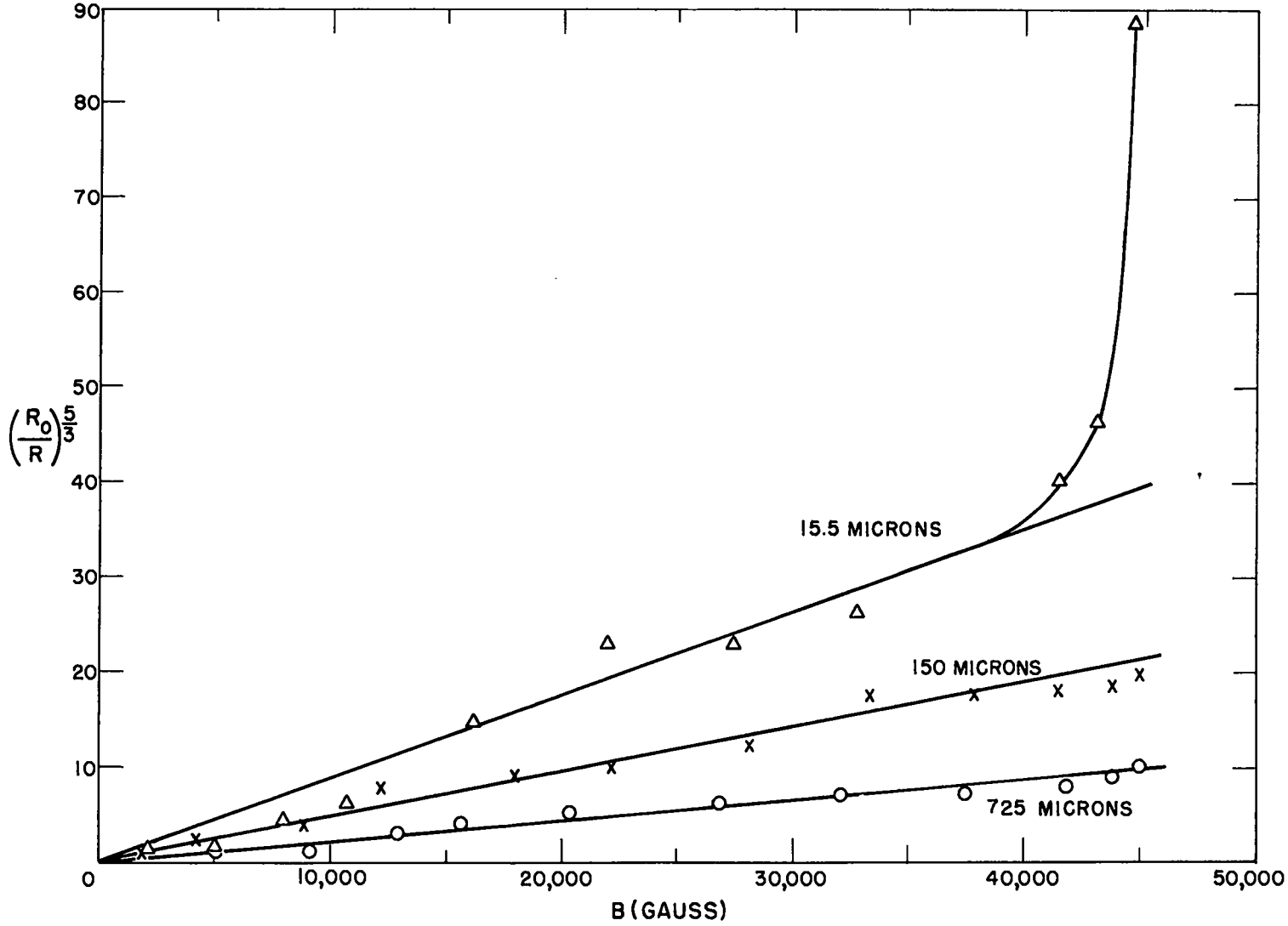

Fig. 13 Plots of $(R_o/R)^{5/3}$ as a function of B for three different values of the initial base deuterium pressure.

pressure, one can estimate the initial and final temperatures for the cases studied.

The results for the curves of Figs. 12 and 13 are given in Table 1.

TABLE 1

TEMPERATURES FOR DIFFERENT INITIAL PRESSURES

Initial Deuterium Pressure (microns)	kT_o (ev)	kT_f (ev)
15.5	13.8	214
123	3.1	41
150	4.2	47
725	4.5	26

The assumption that N_o is the value indicated by the initial deuterium pressure may be in error due to compression behind the shock fronts. But for all the data given here, the main field was excited after the last shock had traveled 10 to 15 cm beyond the region of observation, hence conservation of the total number of particles in the tube would require that the density behind the shock front must have returned to nearly the starting value.

A comparison between the curves of Fig. 13 for 150 and 725 microns is interesting. Their slopes vary by a factor of 2.25. If the initial temperatures are the same, Eq. (9) predicts that these slopes should vary inversely as the square root of the initial density. This ratio is 2.20. These measured predicted values agree within the error of the measurement.

If one considers Curve I, Fig. 12, the average slope in the region 10,000 to 25,000 gauss implies an "effective" initial temperature of about 1 ev by the same analysis. Since for this curve the theory obviously does not hold, and since for this case there may be considerable mixing of the plasma and the B field due to the lack of preheating, the 1 ev value means little except to illustrate that joule heating occurs during the early stages of the compression field due to the secondary current I_θ in the gas.

In Section II, it was predicted, on the basis of shock theory, that the initial temperature kT_o produced by the multiple shocks would be of the order of several electron volts. The measured values of kT_o given in Table 1 are in agreement with this, except for the lowest pressure case, where the 13.8 ev value appears to be about a factor of 2 or 3 higher than one would expect. However, shock velocity measurements at this low pressure were not available, so a comparison cannot be made. The 13.8 ev temperature would correspond to a temperature behind a shock moving at a velocity of about 9.3 cm/μsec in a cold gas. This a reasonable velocity to expect at the lower pressure.

It should be remarked that the magnetic compression studied here is of a somewhat different nature than in the interesting experiment of Kolb,[11] since in his case the initial shock wave was being accelerated by the compression field. Both experiments emphasize the importance of obtaining plasma of high electrical conductivity.

E. Temperature Diffusion

As already mentioned, one of the assumptions of the adiabatic heating theory used here is that there be no loss of heat due to diffusion of temperature along the axis of the magnetic field. The requirement for this to hold is that the magnetic compression must take place rapidly compared to the heat diffusion time.

The heat diffusion is governed by the heat equation:

$$\rho C \frac{dT}{dt} = \nabla \cdot (K \nabla T) \qquad (10)$$

where

T = plasma temperature
C = plasma heat capacity
ρ = particle density
K = thermal conductivity of the plasma
t = time

To solve Eq. (10), we use Spitzer's formula for the thermal conductivity of a fully ionized gas, which states

$$K = a\, T^{5/2} \tag{11}$$

Using (11) in (10), and assuming one-dimensional heat loss as the only source of temperature change, the solution of the heat equation gives

$$t_{1/2} = \frac{b\, L^2 \rho}{T^{5/2}} \tag{12}$$

where

$t_{1/2}$ = time for the temperature to decay to one-half its original value

L = length of the contained plasma, i.e., the diffusion dimension

b = constant of proportionality

The constant b depends on the value of a in Eq. (11), the geometric constant of separation from the solution of Eq. (10), and on the units used for the other quantities. An absolute determination of the constant b is subject to considerable uncertainty, but it is quite reasonable to expect that the heat diffusion time depends on T, ρ, and L in the manner shown by Eq. (12).

In an effort to learn something about the actual diffusion times existing in the experiment, an analysis has been made of one of the smear pictures for which a considerable portion of the cooling quarter cycle following the first heating quarter cycle is visible. The analysis is made as follows: A plot of $(R_o/R)^{5/3}$ versus B is made for both the heating and cooling regions, i.e., for the quarter cycles of increasing and decreasing magnetic field. Straight lines are drawn to average the plotted points, as in Fig. 14. Values of $(R_o/R)^{5/3}$ at each of five field strengths are obtained from the heating and cooling regions, and the time between the equal values of field strength is found. From the change in the ratio $(R_o/R)^2$ for each field strength, an estimate of the loss of temperature during the corresponding time interval can be computed. For example, at

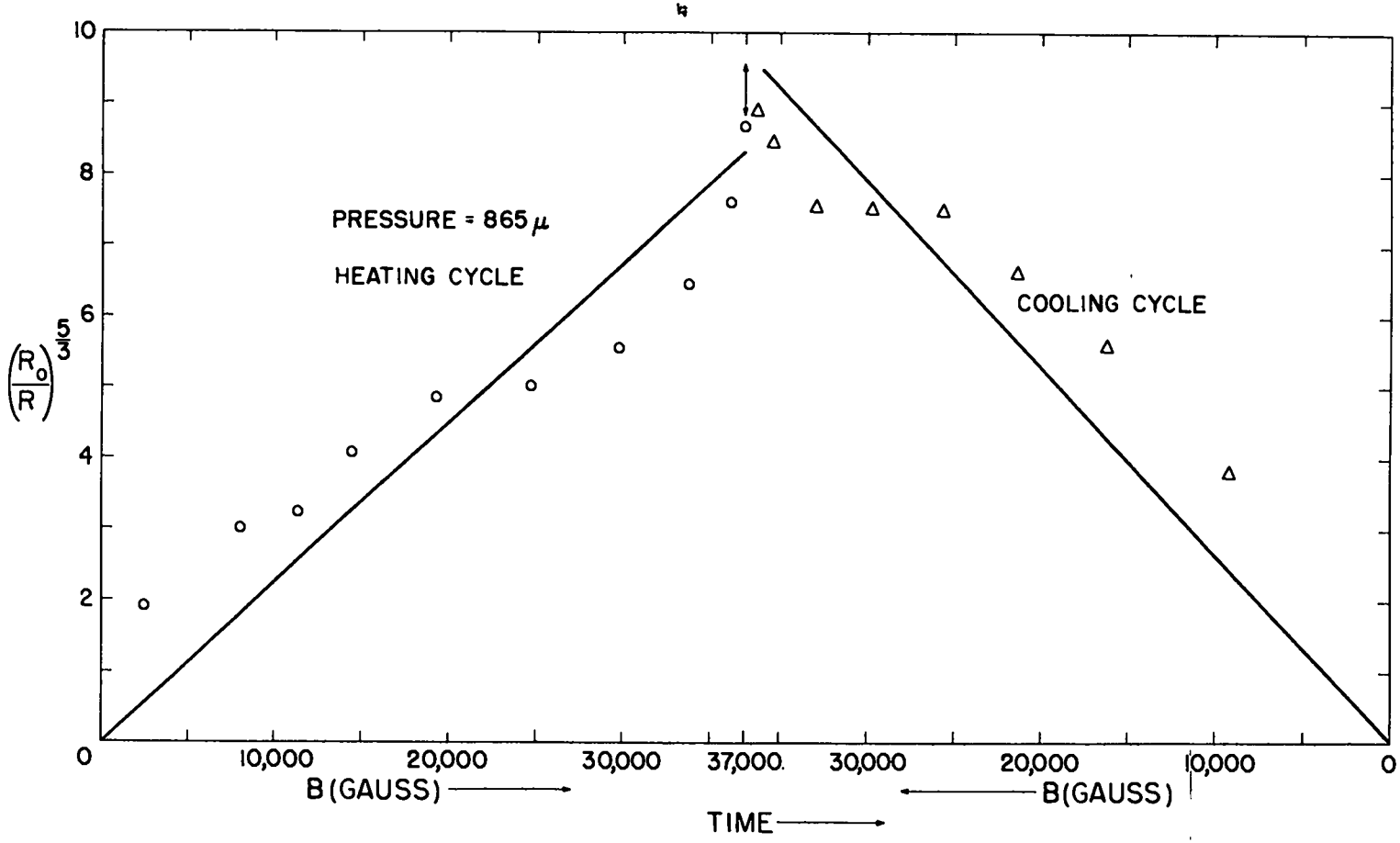

Fig. 14 Plot of $(R_o/R)^{5/3}$ as a function of B for both compression and decompression of the plasma.

a given field strength, a smaller value of R on the cooling cycle than at the same point on the heating cycle indicates a loss of temperature.

From these values, characteristic times $t_{1/2}$ are obtained, as well as the density ratios (ρ/ρ_o) and the temperatures corresponding to each field strength. These numbers, obtained from Fig. 14, are given in Table 2. The values for temperature are based on the value of $T_o = 3.6$ ev given by the slope of the $(R_o/R)^{5/3}$ versus B heating curve. These data are for the case of an initial pressure of 865 microns.

TABLE 2

DENSITY RATIOS, TEMPERATURES, AND CHARACTERISTIC TIMES FOR FIVE FIELD STRENGTHS

B (gauss)	ρ/ρ_o	T (ev)	$t_{1/2}$ (μsec)
5,000	1.12	4.1	30
10,000	2.93	6.3	27.5
20,000	6.05	12.3	17.8
30,000	9.88	17.0	11.1
35,000	11.8	19.4	7.9

Figure 15 shows a plot of $t_{1/2}\ (\rho_o/\rho)$ versus $(T/T_o)^{-5/2}$. The resulting straight line is just what would be expected if Eq. (12) holds, indicating that the heat loss is due to heat diffusion and that thermal conductivity is proportional to $T^{5/2}$.

This result is not at all conclusive since Fig. 15 is based on only one smear picture. It is presented here only to illustrate how additional data on the effect of temperature diffusion might be obtained. A more accurate way to observe temperature diffusion would be to keep the magnetic field constant at one of the higher values of temperature and observe the reduction of plasma radius for as many time intervals as possible.

From the results of Fig. 15 and the proportionalities of Eq. (12), values of $t_{1/2}$ can be calculated for the lower pressure cases. These

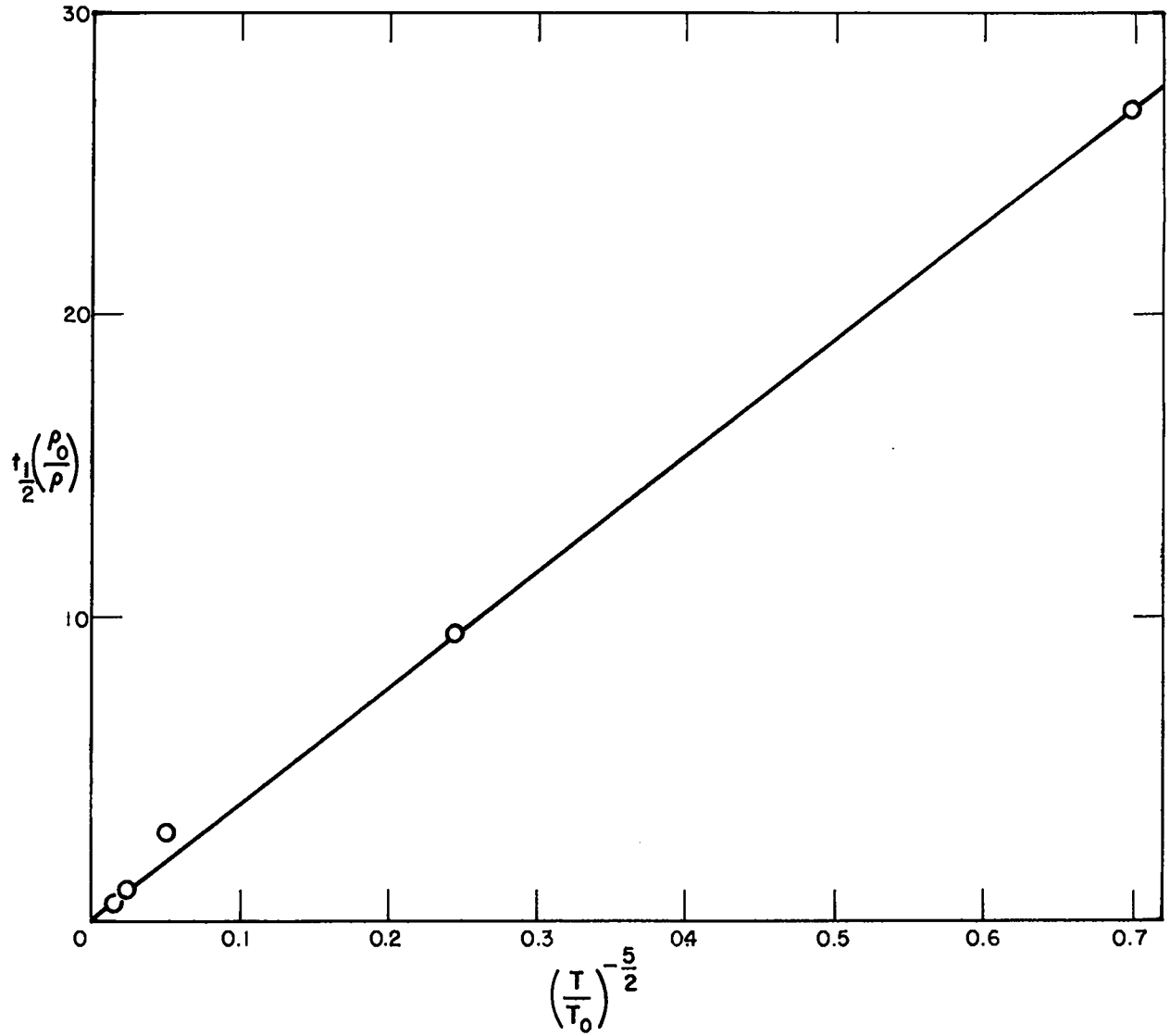

Fig. 15 Plot of $t_{1/2}(\rho_o/\rho)$ versus $(T/T_o)^{-5/2}$.

values indicate that at 725 microns and at 150 microns, the values of $t_{1/2}$ are sufficiently large in comparison with the 10 μsec compression time that heat diffusion will not be serious. The values of $t_{1/2}$ for the 15.5 micron case are much smaller than 10 μsec and indicate that heat diffusion should be even more serious than indicated in Fig. 13, which, however, does indicate considerable heat loss at the high temperature end.

Since Totempole II experiments look most promising at low densities, i.e., one achieves the highest temperatures there, and since heat diffusion increases as $T^{5/2}/N$, the need for a faster rising compression field and a field configuration to reduce end losses is strongly indicated by these results.

IV. Conclusions and Recommendations

The data reported here should be regarded as preliminary and in no way decisive. Much work remains to be done to investigate thoroughly the behavior of the Totempole II device. However, with these limitations in mind, a few conclusions may be drawn regarding Totempole II. The data indicate that:

1. Planar shocks from tapered $\dot{B}_z$ sections can be used to produce a plasma of sufficient temperature to satisfy the minimum preheating requirements of the experiment.

2. The adiabatic heating theory appears to hold over the range of temperatures and pressures studied, except perhaps for the high temperature case at the lowest pressure (15.5 microns) used. This conclusion is based primarily on the linearity of the $(R_o/R)^{5/3}$ versus B curves. This linearity indicates that there is no serious heat loss due to radiation, temperature diffusion, etc., over most of the region tested. Thus Eq. (8) may be used with some confidence to predict the behavior of Totempole II experiments.

3. The high temperature behavior of the 15.5 micron curve of Fig. 13 and the results of Section III E strongly indicate that temperature diffusion becomes serious if one proceeds to lower initial densities or higher final temperatures.

4. The cleanliness of the discharge tube after many dozens of firings strongly suggests that the impurities are reduced by one or more orders of magnitude as compared with systems of comparable energy using electrodes.

5. The long radial containment times and apparent lack of serious diffusion of the plasma into the magnetic field indicate that a considerable electrical conductivity was achieved during the compression stage. A comparison with the magnetic diffusion times of the shock channeling experiment[2] supports the conclusion that Totempole II achieved electron temperatures in excess of 20 to 30 ev.

There seems no reason to doubt that a combination of the following improvements would enable the Totempole II type experiment to produce plasma of sufficient temperature to give significant thermonuclear neutron yields.

(a) The temperature diffusion effect can be reduced by increasing the length (L) of the main compression coil or by a magnetic mirror configuration of the compressing field. A faster rising compressing field is also very desirable.

(b) Equation (8) shows that the final temperature may be increased by increasing the final strength of the compressing field.

(c) Higher initial temperatures (T_o) are desirable both to increase the final temperature as predicted by Eq. (8) and to reduce radial diffusion of the magnetic field into the plasma during the early stages of compression. These higher values of (T_o) can be obtained by increasing the strength of the preheating longitudinal shocks. They might also be obtained by use of "Gloworm"[4] type $\dot{B}_z$ heating and its associated radial shocks. This would involve applying a separate $\dot{B}_z$ of high E_θ superimposed axially on the main compressing field. This $\dot{B}_z$ heating would be fired before the main compressing field. Since the "Gloworm" data indicated temperatures of 5 to 10 ev, this method looks quite feasible. However, one should study it with magnetic probes to verify that mixing of magnetic field and plasma does not become serious during the preheating phase.

(d) Equation (8) also shows that lower initial densities (N_o) would increase the final temperature. However, as one lowers the base pressure of any given device, a point will be reached where impurities from the walls will become appreciable compared to the deuteron density. So any device of this type would have an optimun initial density which should be determined. Since heat diffusion became important in the Totempole II, the optimun base pressure was somewhere near 15 microns.

In addition to the potentialities of producing thermonuclear neutrons, Totempole II type experiments look promising as a means of studying the basic physical properties of hot plasma.

REFERENCES

1. E. M. Little and D. B. Thomson, Los Alamos internal report, June 1957.

2. F. R. Scott, W. P. Basmann, E. M. Little, and D. B. Thomson, "Magnetic Channeling of a Strong Shock," The Plasma in a Magnetic Field, Stanford University Press, Palo Alto, California (1958).

3. J. W. Mather, et al., Los Alamos internal reports, November-December 1953 and January-March 1954.

4. W. M. Bullis and D. B. Thomson, Los Alamos internal reports, November-December 1956.

5. V. Josephson, "Production of High Velocity Shocks," J. Appl. Phys. 29, 30-32 (1958).

6. R. B. Ferrell, Los Alamos Scientific Laboratory; private communication, January 1957.

7. R. B. Ferrell and D. B. Thomson, Los Alamos internal reports, June-July 1955.

8. F. R. Scott, "Totempole," Berkeley Conference on Thermonuclear Reactions, TID-7536, Pt. II, February 1957.

9. Burkhardt, Dunaway, Mather, Phillips, Sawyer, Stratton, Stovall, Jr., and Tuck, J. Appl. Phys. 28, 519-521 (1957).

10. Lyman Spitzer, Jr., Physics of Fully Ionized Gases, pp. 76-81, Interscience Publishers, Inc., New York, 1956.

11. A. C. Kolb, "Propagation of Strong Shock Waves in Pulsed Longitudinal Magnetic Fields," Phys. Rev. 107, 1197 (1957).